

TAPERING STUDIES FOR TW LEVEL X-RAY FELS WITH A SUPERCONDUCTING UNDULATOR AND BUILT-IN FOCUSING*

C. Emma, C. Pellegrini, UCLA, Los Angeles, CA 90095 USA
K. Fang, J. Wu, SLAC, Menlo Park, CA 94025, USA

Abstract

Tapering optimization schemes for TeraWatt (TW) level X-ray Free Electron Lasers (FELs) are critically sensitive to the length of individual undulator and break sections. Break sections can be considerably shortened if the focusing quadrupole field is superimposed on the undulator field, increasing the filling factor and the overall extraction efficiency of the tapered FEL. Furthermore, distributed focusing reduces the FODO length and allows one to use smaller beta functions, reducing particle de-trapping due to betatron motion from the radial tails of the electron beam. We present numerical calculations of the tapering optimization for such an undulator using the three dimensional time dependent code GENESIS. Time dependent simulations show that 8 keV photons can be produced with over 3 TW peak power in a 100m long undulator. We also analyze in detail the time dependent effects leading to power saturation in the taper region. The impact of the synchrotron sideband growth on particle detrapping and taper saturation is discussed. We show that the optimal taper profile obtained from time independent simulation does not yield the maximum extraction efficiency when multi-frequency effects are included. A discussion of how to incorporate these effects in a revised model is presented.

INTRODUCTION

In this work we analyze the tapering optimization of a high efficiency [1] TW-level X-ray FEL using time independent and time dependent GENESIS simulations. We show that the solution obtained for the optimal taper profile in time independent simulations does not yield the maximum extraction efficiency when fully time dependent physics is included in the dynamics of the the electron beam and radiation field system. We study the optimization for a superconducting, 2 cm period, helical undulator with built in focusing. This undulator design is optimized for maximum efficiency, reduction of intra module undulator length, strong transverse focusing, short gain length and minimum total undulator length.

UNDULATOR DESIGN

We apply the tapering optimization method [2] to an undulator designed specifically to achieve TW power X-ray pulses in the shortest possible undulator length. Our ideal undulator is superconducting, with a short 2 cm period and a peak on axis field B_0 of 1.6 T. For a double helix bifilar magnet with equal and opposite currents this field is given

Table 1: GENESIS Simulation Parameters

Parameter Name	Parameter Value
Beam Energy	12.975 GeV
Peak Current	4000 A
Normalized Emittances	0.3/0.3 $\mu\text{m rad}$
Average beta function	5 m
RMS Energy Spread	10^{-4}
Bunch Length	6 fs
Seed radiation power	5-25 MW
Radiation Wavelength	1.5 \AA
Rayleigh Length	10 m
Undulator Period	2 cm
Undulator Parameter	3
Quadrupole Focusing Strength	26.4 T/m
Undulator Section Length	1 m
Undulator Break Length	20 cm
FEL parameter	1.66×10^{-3}
3-D Gain Length	65 cm

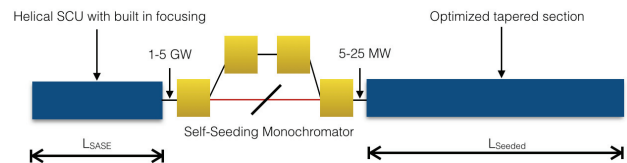


Figure 1: Schematic of the undulator for hard X-ray multi TW peak power output, designed to achieve high extraction efficiency in the shortest possible distance.

by [3]:

$$B_0 = \frac{4k_u I}{10^5} [k_u a K_0(k_u a) + K_1(k_u a)], \quad (1)$$

where I is the current in the coils, $k_u = 2\pi/\lambda_u$ is the undulator wavenumber, a is the helix radius and K_0 and K_1 are modified Bessel functions. For a helical bore radius $a = 7.5$ mm the total current required through the coils is $I = 484$ A which, considering coils of $\sim \text{mm}^2$ surface area, gives a current density below the critical value for superconducting NbTi or Nb₃Sn wires. From the point of view of operation a superconducting undulator has advantages such as resistance to radiation damage and reduced sensitivity to wakefields, for a more detailed description see Ref. [4]. The undulator is helically polarized as this increases the effect of refractive guiding in the post-saturation regime and improves the FEL performance [5].

* Work supported by: DOE Grant Number DE-SC0009983

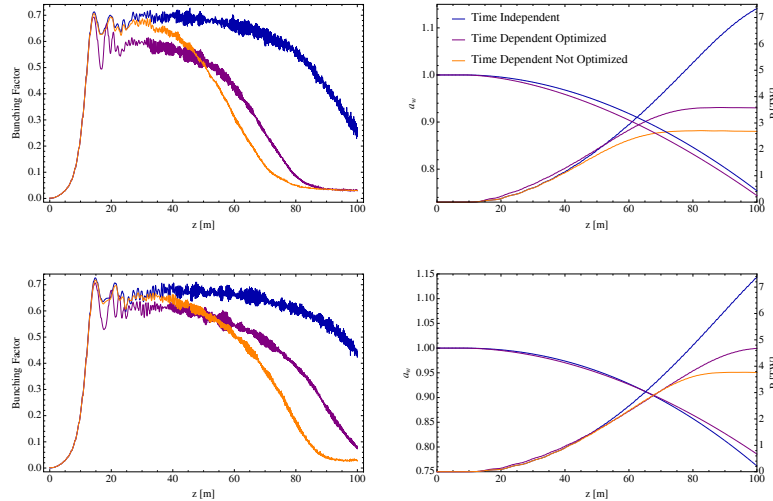


Figure 2: Bunching factor (left), taper profiles and FEL radiation power evolution (right) obtained from time independent and time dependent optimization. The top plots correspond to an input energy spread $\sigma_{E,0}=3.1$ MeV consistent with the SASE result from Fig. 1. The bottom plots are an alternate case with $\sigma_{E,0}=1.5$ MeV. In both cases $z=0$ is after the self-seeding monochromator and the input seed power is 5 MW.

In order to accommodate diagnostics a realistic undulator design must include periodic break sections, with longer breaks adversely affecting performance. This is due essentially to three effects. Firstly, diffraction effects are critical to the performance of a tapered FEL particularly for long, multiple Rayleigh length undulators. While these effects are mitigated by refractive guiding inside the undulator, there is no guiding during the break sections and the radiation size increases exponentially, reducing the field amplitude, causing particle detrapping and limiting the extraction efficiency. Secondly, a break of length L_b introduces a phase error $\Delta\Psi \sim L_b\delta/\gamma^2 = 2n\lambda_r\eta$ for a particle with relative energy offset $\eta = \delta\gamma/\gamma_r$ with respect to the resonant particle. Thus longer break sections increase electron phase mixing and reduce the bunching factor. Finally as a practical consideration, for a given total undulator length, longer break sections reduce the length of magnetic elements limiting the electron deceleration and over-all extraction efficiency. To minimize the break length we superimpose the focusing quadrupole field on the helical undulator field, similar to the design successfully tested in Ref. [6]. One advantage of distributed quadrupole focusing is the possibility to operate at small betatron beta function, due to the reduced FODO lattice length L_f . This minimizes the transverse beam envelope oscillation $\Delta\beta^2/\beta_{av}^2 = \beta_{av}L_f/(\beta_{av}^2 - L_f^2)$ which also degrades the FEL performance [7]. In our study the undulator magnetic field is tapered continuously and the section length is chosen to be 1 m, close to the 3-D gain length with 20 cm breaks in between.

Although this kind of undulator has never been constructed in the past, the parameters presented in this design are similar to what is currently being considered for an LCLS-II-like planar superconducting undulator with the addition of built in quadrupole focusing [4]. A full engineer-

ing and tolerance study of this undulator is needed before we can be confident that it is a feasible option for future high efficiency X-ray FEL facilities.

TAPERING OPTIMIZATION

Time Independent

We first obtain the optimal taper profile, maximizing the output power for a fixed 100 m undulator length in time independent simulations using the three dimensional FEL particle code GENESIS. The tapering law is written as:

$$a_w(z) = a_{w0} \times (1 - c \times (z - z_0)^d), \quad (2)$$

where the parameters z_0, c, d are obtained by multidimensional scans which maximise the output power. The quadrupole focusing can also be tapered to further increase the extraction efficiency as shown in Ref. [2] but that will not be considered in this study. The optimal taper profile obtained from time independent optimization is shown in Fig. 3. The tapering order is approximately quadratic, which follows qualitatively from the fact that in time independent simulations the bunching factor and trapping fraction remain nearly constant in the tapered section and the dominant radiative process is coherent emission. The peak output power is 7.3 TW with an extraction efficiency of 14%. It is important to note that there is no sign of the taper power saturating in the time independent case, which is not the case when time dependent effects are included.

Time Dependent Optimization

Using the optimal taper starting point obtained from time independent simulations, we perform time dependent scans over the taper order d and the taper strength $\Delta a_w/a_w =$

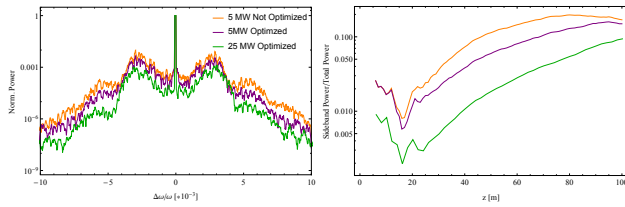


Figure 3: (left) Spectrum at half the undulator length and fractional sideband power (right) for the time independent optimized case and fully time dependent optimized for 5 MW and 25 MW input seed power and 1.5 MeV energy spread. Sideband power grows faster in the time independent optimized case, leading to particle detrapping and early saturation of the tapered FEL.

$c \times (L_w - z_0)^d$. As shown in Fig. 3, the values of the taper order and taper strength yielding the maximum power in time independent simulations are not the optimal choice of parameters once time dependent effects are included. The variation in peak power is more sensitive to variations in the taper profile in the time dependent cases. The optimal taper order is weaker than quadratic, and is reduced compared to the time independent case. This is due to the FEL increased sensitivity to particle detrapping when electron beam shot noise and multiple frequency effects are included.

Since the coherent emission power is proportional to the product of the number of trapped particles and the change in resonant energy (taper strength), a slower taper preserves the trapping for longer, maximising the product and the overall extraction efficiency. In the large energy spread case it is important to note that the time dependent optimized taper profile has a slower taper order but a larger over-all deceleration rate. This results in a worse particle capture in the early stages of the tapered section ($z=10-50$ m) but a reduction in detrapping in the remainder of the undulator. This can be understood by examining the functional form for the resonant phase:

$$\sin \Psi_R(z) = \chi \frac{|a'_w(z)|}{E(z)} \quad (3)$$

where $\chi = (2 * m_e * c^2 / e)(\lambda_w / 2\lambda_s)(1/\sqrt{2}[JJ])$ is a constant independent of z and $E(z)$ is the electric field amplitude. The time dependent optimized taper reduces $|a'_w(z)|$ in the second half of the undulator $z=50-100$ m, maintaining a larger bucket area in the region where the amplitude of the sidebands is more appreciable and the system is more sensitive to detrapping. From this it is clear that a fully optimized form of the taper profile should have an improved capture rate in the early stages with a profile similar to what one obtains from time independent optimization, and a slower decrease in the undulator field in the later stages when time dependent effects are more appreciable. This requires a more elaborate functional form for $a_w(z)$ and will be investigated in future work.

SIDEBAND INSTABILITY

The mechanism of sideband generation and amplification in free electron lasers can be summarized as follows [8]. Firstly, sidebands are generated due to amplitude and phase modulations of the electric field, due to the trapped particles undergoing synchrotron oscillations as they pass through the undulator. Using Maxwell's equations in the 1-D slowly varying envelope approximation we can write the evolution of the electric field amplitude and phase [8]:

$$a'_s = \frac{\omega_p^2}{2\omega_s c} a_w \left\langle \frac{\sin \Psi}{\gamma} \right\rangle \quad (4)$$

$$\delta k_s = \frac{\omega_p^2}{2\omega_s c} \frac{a_w}{a_s} \left\langle \frac{\cos \Psi}{\gamma} \right\rangle \quad (5)$$

where a_s is the dimensionless vector potential for the electric field, ω_p is the electron beam plasma frequency and Ψ is the ponderomotive phase. It is clear from these that as the electrons oscillate in the longitudinal phase space (Ψ, γ) the gain and the phase shift of the radiation field will be different at different locations in the undulator and, due to shot noise in the electron beam, at different locations along the bunch. This results in a temporal modulation of the radiation field giving rise to sidebands displaced from the central wavelength by a quantity proportional to the synchrotron period:

$$\lambda_{s'} \approx \lambda_s \left[1 \pm \frac{\lambda_w}{L_{sy}} \right] = \lambda_s \left[1 \pm \left(\frac{a_w a_s}{1 + a_w^2} \right)^{1/2} \right] \quad (6)$$

where L_{sy} is the synchrotron period. Once the sidebands are generated, the electron oscillations are driven by a multiple frequency ponderomotive potential, therefore the equations of motion and Maxwell's equations for the electric field, must be modified accordingly. An analysis of the simplest two frequency model shows that the coupled beam-radiation system is unstable and that the sideband amplitude will grow from noise for any realistic electron distribution [8]. When the strength of the sidebands exceeds a critical level, electron motion becomes chaotic leading to severe particle detrapping and a loss of amplification of the FEL signal [9]. Thus, as has been discussed by previous authors, suppressing the sideband instability is the key issue for tapered FEL designs [1], particularly those which are multiple synchrotron periods in length.

As is shown in Fig. 4 the time dependent optimized taper profile reduces sideband amplitude growth. This results in a reduction in particle loss and a delayed taper saturation, both evidenced in the increased bunching factor and output power in Fig. 2. In the simple case of constant sideband and carrier amplitude the diffusion coefficient caused by sideband excitations is proportional to the ratio of the power in the sidebands to the power in the FEL signal $D \propto CP_{s'}/P_s$ with the coefficient C depending on the type of sideband spectrum [9]. As is also shown in Fig. 4 this is reduced in the time dependent optimized case. The peak power improves

by 1 TW between the time dependent optimized and un-optimized cases, an overall improvement of 2 %. Despite the dedicated time dependent optimization we do not recover the single bucket extraction efficiency unlike results previously reported in Ref. [10].

CONCLUSION

In this paper we perform the first comparison of time independent and time dependent tapering optimization for a high efficiency seeded hard X-ray FEL. The comparison is done for an undulator design optimized to achieve TW peak powers in the shortest possible distance: helical, superconducting and with built-in focusing. We demonstrate that the taper profile yielding the maximum power in time independent optimizations does not correspond to the optimal solution when time dependent effects are included in the simulation. By performing time dependent scans of the taper order and the taper strength we show that the maximum output power in time dependent mode is achieved with a lower taper order compared to the time independent case. The difference is due to the increased sensitivity to particle detrapping in the time dependent case, mitigated by a slower taper profile in the later stages of the undulator where time dependent effects are more important. For an input energy spread of 3.1 MeV the final output power increases from 2.7 TW with the time independent taper profile to 3.7 TW with the profile obtained from dedicated time dependent scans.

We have also discussed the importance of the trade-off between energy spread and seed power at the entrance of the tapered undulator section. We show that using a “fresh bunch” with input energy spread of 1.5 MeV determined only by the linac we can decrease particle detrapping, maintain a larger bunching factor and improve the over-all performance. For the same seed power of 5 MW the maximum output power is 4.7 TW after the dedicated time dependent optimization. In a double-bunch system the input seed power can be larger without affecting the input energy spread. We have studied an optimal case with a 25 MW seed and 1.5 MeV energy spread and found that the output power reaches 6.3 TW at the end of the undulator, a 12 % efficiency which approaches the time independent result of 7.7 TW.

We identify the sideband instability as the fundamental time dependent effect which is not taken into account in time independent optimizations and limits the extraction

efficiency by causing particle detrapping. Analyzing the fraction of energy in the sidebands in the $\sigma_E = 1.5$ MeV case with a 5 MW seed, we show that the fraction of energy deposited in the sidebands is below 10 % for 70 m in the time dependent optimized taper profile while it exceeds 10 % after 40 m in the the time independent case reaching 14 % towards the end of the undulator.

While extending the simulation method of Ref. [2] to include time dependent effects significantly improves the performance of tapered X-FELs the current procedure is both time consuming and simulation intensive. The form of the taper profile $a_w(z)$ needs a more complicated functional dependence to optimize trapping in the early stages and reduce sideband growth in the later stages where time dependent effects play a more important role. With the enhanced understanding gained of the critical parameters limiting performance, such as the growth of the sideband instability, an improved algorithm can be developed which acts to directly suppress these effects. Such a scheme will be developed in future work.

REFERENCES

- [1] N.M. Kroll, P.L. Morton, M. Rosenbluth, IEEE Journal of Quantum Electronics, vol. 17, p. 1436, 1981
- [2] Y. Jiao et al., Phys. Rev. ST. AB., vol. 15, p. 050704, 2012
- [3] W.R. Smythe, 1950, Static and Dynamic Electricity (McGraw-Hill, New York), p. 277.
- [4] P. Emma et al., in FEL 2014 Conference proceedings, Basel, Switzerland, p. THA03, 2014.
- [5] D. Prosnitz, A. Szoke, V.K. Neil, Phys. Rev. A, vol. 24, p. 1436, 1981
- [6] A. Murokh et al., Nuclear Instruments and Methods in Physics Research Section A: Accelerators, Spectrometers, Detectors and Associated Equipment, vol. 507, no. 12, pp. 417-421, 2003.
- [7] S. Reiche and E. Prat, in FEL 2012 Conference proceedings, Nara, Japan, p. MOOC02, 2012.
- [8] N.R.M. Kroll, in Free Electron Generators of Coherent Radiation, pp. 147-174, Springer Berlin Heidelberg, 1979.
- [9] S. Riyopoulos and C. M. Tang, Physics of Fluids, vol. 31, no. 11, pp. 3387-3402, 1988.
- [10] B. Hafizi, A. Ting, P. Sprangle, and C. M. Tang, Physical Review A, vol. 38, no. 1, 1988.